Mechanistic Studies of Permeation Enhancers

7

S. Kevin Li and William I. Higuchi

Contents

S.K. Li (✉)
Division of Pharmaceutical Sciences,
College of Pharmacy, University of Cincinnati,
3225 Eden Ave, Rm 160, Cincinnati,
OH 45267-0004, USA
e-mail: kevin.li@uc.edu

W.I. Higuchi
Pharmaceutics and Pharmaceutical Chemistry,
College of Pharmacy, University of Utah,
30 S 2000 E, Skaggs Hall, Salt Lake City,
UT 84112, USA

7.1 Introduction

Most of the chemical permeation enhancer studies in the past decades have been aimed at gaining better insights into the relationship between the nature of the enhancers and their effectiveness in permeation enhancement. In typical in vitro studies of chemical permeation enhancers, the enhancer in question is usually applied with a drug in solution or suspension to one side of the membrane, and the effectiveness of the enhancer compared to a control is determined by the rate of transport of the drug. Under this approach, the different relationships among the enhancer molecular structures and their effects as permeation enhancers have been studied (e.g., reviewed in Lee et al. 1991; Smith and Maibach 1995; Hadgraft 2001).

Our laboratory has been studying the mechanism of action of permeation enhancers for more than a decade. A different experimental approach has been employed in these studies (Kim

© Springer-Verlag Berlin Heidelberg 2017

N. Dragicevic, H.I. Maibach (eds.), *Percutaneous Penetration Enhancers Drug Penetration Into/Through the Skin*, DOI 10.1007/978-3-662-53270-6_7

et al. 1992; Yoneto et al. 1995; Warner et al. 2003; He et al. 2004). First, if mechanistic insight is to be collected directly, a symmetric and equilibrium configuration (with respect to the enhancer) should be used. In the symmetric configuration, the enhancer is present at equal concentrations in both the donor and receiver chambers of a side-by-side diffusion cell and in equilibrium with the membrane. Under these conditions, the complications arising from enhancer concentration (or activity) gradients across the membrane (Liu et al. 1991, 1992; Chantasart and Li 2010) can be avoided. These enhancer gradients would otherwise lead to a situation in which the local permeation enhancement varies with the position within the membrane and make mechanistic data analysis difficult. With the symmetric configuration, the permeability coefficients obtained for the permeants can be used directly to determine the effectiveness of an enhancer in enhancing transdermal transport (enhancer potency). Second, good enhancers are usually lipophilic and relatively water-insoluble. Because they are water-insoluble, well absorbed, and need to be solubilized for effective presentation, they cannot be systematically investigated conveniently for structure–enhancement activity. Establishing equilibrium between the enhancer and the membrane is therefore necessary in obtaining mechanistic insights into the action of permeation enhancers and for establishing a structure–enhancement relationship. Third, model analyses to separate the effects of permeation enhancement on transport across the lipoidal and pore transport pathways using model permeants of different polarity have been used. The effects of the enhancers upon the intercellular lipoidal and pore pathway transport have been delineated in order to understand the mechanism of action of the enhancers. Last, in the assessment of skin permeation enhancement, changes in the chemical potential (activity) of the permeant in the enhancer solution with respect to that in the buffer solution (the control) are corrected for, so the effects of permeant activity alteration upon transport in the presence of the enhancers are taken into account. Taking the above issues into consideration, we have developed a research strategy to gain mechanistic insights into the effects of enhancers upon transport across skin, to determine the intrinsic potencies of the enhancers, and to establish a quantitative structure–enhancement relationship between the enhancers and permeation enhancement. This chapter is a review of our studies employing this strategy and the experimental approaches.

7.2 Methods

7.2.1 Animal Model

Experiments were conducted with freshly separated hairless mouse skin (HMS) obtained from the abdomen region and freed from adhering fat and other visceral debris. HMS was selected as the model for human skin for the following reasons. HMS has relatively constant lipid content (Yoneto et al. 1998), and a large body of HMS data is available in the literature allowing the direct comparisons of our results with those in previous studies. HMS stratum corneum (SC) lipid composition (Grubauer et al. 1989) is also similar to that of human skin (Lampe et al. 1983). In certain cases, such as for experiments requiring long-term skin stability in aqueous solution, HMS is not a good model of human skin (Lambert et al. 1989). However, in the investigation of chemical permeation enhancers for the lipoidal pathway and where relatively short experimental times are involved, HMS can be an adequate quantitative model for human skin (Kim et al. 1992; Li et al. 1997). For example, Chantasart et al. (2007) compared the effects of permeation enhancers on the permeability coefficients of the lipoidal pathways of HMS and human epidermal membrane (HEM) under the symmetric and equilibrium configuration. The quantitative structure–enhancement relationships of the enhancers in HMS and HEM were also compared. The results suggest that for the assessment of skin permeation across the lipoidal pathway and for the mechanistic studies of the effects of skin permeation enhancers upon this pathway, HMS can be a reliable model for human skin. There is no direct evidence of significant discrepancies between the mechanisms of action of permeation enhancers in HMS and human skin.

7.2.2 Transport Experiments

7.2.2.1 Permeability Coefficient Determination

The permeability experiments were carried out as previously described with a two-chamber side-by-side diffusion cell in phosphate buffered saline (PBS) at 37 °C (Yoneto et al. 1995; Warner et al. 2003). Each compartment has a 2-mL volume and an effective diffusional area of 0.67 cm^2. The skin membrane was sandwiched between the two half cells and an enhancer solution in PBS was pipetted into both chambers. A list of the enhancers investigated is shown in Fig. 7.1. To attain equilibrium of the enhancer with the HMS, the enhancer solution in both diffusion cell chambers was replaced until the SC was essentially in equilibrium with the enhancer solution (enhancer/PBS). With highly hydrophobic enhancers (e.g., 1-dodecyl-2-pyrrolidone), due to the extensive depletion of the enhancers in the aqueous phase that made it difficult to achieving an equilibrium of the enhancers between the aqueous phase and the SC at the target concentrations, an aqueous reservoir system (enhancer solubilizing system of micelles or cyclodextrin) that neither significantly interacts with the SC nor acts as a permeation enhancer was used (Warner 2003; Shaker et al. 2003; Warner et al. 2008). The concentrations of the enhancers in the diffusion cell chambers were frequently checked by HPLC or GC. The loss or depletion of all the enhancers was less than 5 % in most cases and less than 15 % in the extreme case at the end of the transport experiments.

Corticosterone (CS) was the main model permeant. Estradiol (ES) and hydrocortisone (HC) were the two other steroidal permeants tested in the studies. Other permeants used will be discussed in the section on "Effects of Permeation Enhancement on Permeants of Different Molecular Sizes." The steroidal permeant at radiotracer levels and at concentrations far below its solubility was added to the donor chamber following enhancer equilibration. Samples were withdrawn from the donor and receiver chambers at predetermined time intervals and analyzed. Permeability experiments with model ionic polar permeant tetraethylammonium ion (TEA) were conducted in essentially the same manner. The total permeability coefficients (P_T) were determined from data obtained under steady-state conditions (experiment time points around three to five times longer than the lag times). The permeability coefficient of the dermis–epidermis combination ($P_{D/E}$) was obtained in the same manner, but the skin was stripped 30 times with 3 M Scotch tape prior to excision and assembly into the diffusion cell.

Another method to evaluate the potency of permeation enhancers, particularly highly lipophilic enhancers, is the direct equilibration of the skin with liquid enhancers and the subsequent skin transport experiments with PBS as the donor and receiver solution in a side-by-side diffusion cell in the absence of cosolvents or solubilizing agents (Ibrahim and Li 2009a, b). With highly lipophilic enhancers, the depletion of the enhancers from the skin to the aqueous solution in the diffusion cell chambers is expected to be minimal, and essentially constant enhancer concentration can be maintained in the SC over the duration of the permeability experiments. This method was recently used to study the structure–enhancement relationship of highly lipophilic chemical enhancers and evaluate enhancer effectiveness under the condition when the SC was saturated with the enhancer at thermodynamic activity equivalent to its pure state (i.e., at the solubility of the enhancer in the SC lipids). A disadvantage of this approach is the inability to control the enhancer concentration in the diffusion cell chamber (i.e., always at saturation in the aqueous solution) and hence in the skin. In other words, this approach cannot be used to evaluate the effects of enhancer concentration upon skin permeation enhancement. Permeation enhancer studies using this approach (Ibrahim and Li 2009a, b; Chantasart and Li 2012) will not be discussed in this chapter but have been discussed in a recent book chapter (Li and Higuchi 2015).

7.2.2.2 Reversibility Study

Diffusion cells were assembled with full thickness HMS as described for a typical permeation experiment under the symmetric and equilibrium

Fig. 7.1 Chemical structures of the enhancers. R, R' = alkyl chain

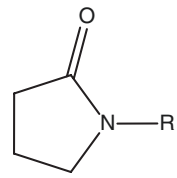

1-alkyl-2-pyrrolidones (AP)

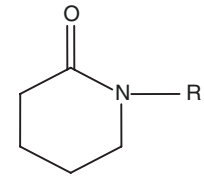

1-alkyl-2-piperidinones (API)

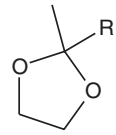

2-(1-alkyl)-2-methyl-1,3-dioxolanes (MD)

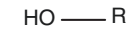

1-alkanols (AL)

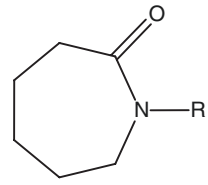

1-alkyl-2-azacycloheptanones (AZ)

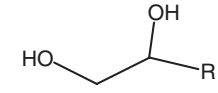

1,2-alkanediols (AD)

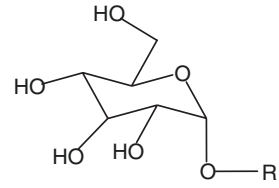

n-alkyl-β-D-glucopyranosides (AG)

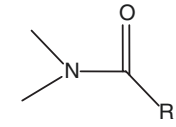

N,N-dimethyl alkanamides (AM)

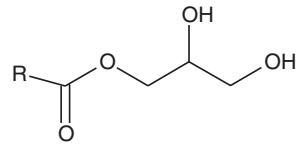

1,2-dihydroxypropyl alkanoates (MG)

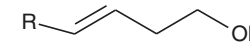

trans-3-alken-1-ols (TAL)

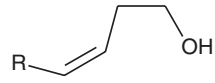

cis-3-alken-1-ols (CAL)

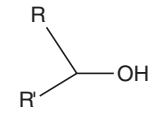

Branched alkanols (bAL)

configuration, and equilibrium between the membrane and the enhancer solution was allowed to take place. However, in this protocol, both chambers of the diffusion cell were then rinsed with PBS to remove the enhancer equilibrated in the membrane. Following the PBS rinsing regime, transport studies were carried out with PBS in both chambers. The permeability coefficients obtained with PBS after pretreatment with enhancers were then compared with those obtained with pretreatment with PBS only. Except for the highly lipophilic enhancers, all enhancers were tested for reversibility at enhancer concentrations up to enhancement factor (E) at $E = 10$ (Warner et al. 2001, 2003; He et al. 2003, 2004; Chantasart et al. 2004), and their effects upon permeation across SC were shown to be essentially reversible (permeability coefficients in PBS after enhancer pretreatment were within a factor of 2 of those in PBS without enhancer pretreatment).

7.2.2.3 Model Description and Analysis of Experimental Data

The permeability coefficient (P) of a probe permeant was calculated according to Eq. (7.1) (Warner et al. 2001):

$$P = \frac{1}{AC_D}\frac{dQ}{dt} \tag{7.1}$$

where A is the diffusional area of the diffusion cell, C_D is the concentration in the donor chamber, and dQ/dt is the slope of the linear region of the cumulative amount of permeant in receiver chamber (Q) vs. time plot.

Total permeability coefficient expression for full-thickness skin is written as follows:

$$P_T = \frac{1}{\frac{1}{P_{SC}} + \frac{1}{P_{D/E}}} \tag{7.2}$$

where P_{SC} is the permeability coefficient for the stratum corneum (SC) and $P_{D/E}$ is the permeability coefficient for the epidermis-dermis combination (D/E) and can be obtained from experiments of tape-stripped skin. P_{SC} can be further divided into parallel lipoidal and pore pathway components in SC via the following equation:

$$P_{SC} = P_L + P_P \tag{7.3}$$

where P_L and P_P are the permeability coefficients for the lipoidal pathway and the pore pathway (TEA is used as the probe permeant for estimating the magnitude of P_P), respectively, in the SC. The intercellular lipid domain in SC is generally accepted as the lipoidal transport pathway across SC. Substituting Eq. (7.3) into Eq. (7.2) yields:

$$P_T = \frac{1}{\frac{1}{P_L + P_P} + \frac{1}{P_{D/E}}} \tag{7.4}$$

Based on the results from previous studies, the use of CS as the probe permeant allows Eq. (7.4) to be approximated by:

$$P_T \approx P_L \tag{7.5}$$

For other steroidal permeants, P_L can be calculated by Eq. (7.4) with $P_{D/E}$ and P_P values obtained from transport experiments with stripped skin and TEA, respectively. The equation for the lipoidal pathway transport enhancement factor (E) is:

$$E = \frac{P_{L,X}}{P_{L,O}}\frac{S_X}{S_O} \tag{7.6}$$

where $P_{L,X}$ and $P_{L,O}$ are the permeability coefficients for the lipoidal pathway when the solvent is enhancer/PBS and PBS, respectively, and S_X and S_O are the permeant solubilities in enhancer/PBS and in PBS, respectively. The solubility ratio corrects for any activity coefficient differences between the activity coefficient in PBS and that in the enhancer solution. Use of the solubility ratio assumes that Henry's law is obeyed for the permeant in both PBS and enhancer solutions (Kim et al. 1992).

7.2.2.4 Permeant Solubility Determination

The solubilities of the steroidal permeants in PBS and the enhancer solutions were determined by adding excess crystals of the permeant into the

enhancer solution in Pyrex culture tubes. The drug suspension was shaken for 72 h at 37 °C. The culture tubes were then centrifuged for 15 min at 3500 rpm, and the clear supernatants were analyzed for permeant concentrations with HPLC.

7.2.2.5 Determination of Partition Coefficient in Bulk Organic Solvent/PBS Systems

Organic solvent/PBS partition coefficients were obtained at the aqueous enhancer concentrations corresponding to $E=10$ and at one tenth of the $E=10$ concentration, the latter to test whether Henry's law is obeyed in the two liquid phases. The two-phase systems were maintained at 37 °C for 72 h. Both the organic and aqueous phases were centrifuged, and aliquots were carefully withdrawn from both phases and appropriately diluted for subsequent analysis using HPLC or GC.

7.2.3 Partition Experiments

7.2.3.1 n-Heptane Treatment and SC preparation

Before SC preparation, HMS was rinsed with heptane for 3×10 s to remove the SC surface lipids. This rinsing protocol (the number of rinses and the rinse time) was shown to remove approximately 20 % of the SC lipids but did not disrupt the SC barrier (He et al. 2003). Similar treatments with nonpolar organic solvent were also shown to remove skin surface lipids (e.g., Abrams et al. 1993; Nicolaides 1974). SC was then prepared according to the method described by Kligman and Christophers (1963) and Yoneto et al. (1998). Briefly, the skin was placed, dermis side down, on a filter paper (quantitative filter paper No. 1, Whatman®) mounted on a Petri dish. The Petri dish was filled with 0.2 % trypsin in PBS solution up to the surface of SC. The Petri dish was covered and maintained at 37 °C for 16 h. When the skin membrane was placed in distilled water after the trypsin treatment, the dermis and viable epidermal layers would separate and fall away from the SC. The SC was then rinsed with distilled water several times and swabbed with Kimwipe® tissue paper to remove excess water. Then, the SC was placed on aluminum foil and dried at room temperature. After drying, the SC was kept in a freezer for later use.

7.2.3.2 HMS SC Delipidization

Heptane-treated HMS SC samples were prepared as described in the previous section. The delipidized HMS SC was prepared according to the method described previously (Yoneto et al. 1998). Briefly, dried *n*-heptane-treated SC samples (about 1–2 mg) were weighed and transferred into 5 mL $CHCl_3$/MeOH (2:1) mixture and equilibrated for 48 h at room temperature. The residue of SC was then rinsed several times with fresh $CHCl_3$/MeOH (2:1) mixture and dried under room temperature for 24 h. The dried residue was carefully weighed and used for the partition experiments.

7.2.3.3 Partition Experiments with Heptane-Treated and Delipidized HMS SC

Partition experiments were carried out to determine the uptake amounts of the chemical permeation enhancer and of probe permeant ES into *n*-heptane-treated or delipidized HMS SC. Two different partition experimental setups were used in our laboratory. The old setup used a Franz diffusion cell (Yoneto et al. 1998) and would not be discussed here. The following is a brief description of the other method (Chantasart et al. 2004). Heptane-treated SC (about 1–2 mg) or delipidized SC sample was carefully weighed and equilibrated in about 20 mL of enhancer solution ($E=10$ concentration) containing trace amounts of radiolabeled ES (^{3}H-ES) in a screw-capped glass vial. The vial was sealed with parafilm to prevent enhancer solution evaporation and put in a water bath with shaking at 37 ± 0.1 °C for 12 h. The 12-h incubation period was chosen because preliminary studies showed that equilibrium of enhancer and ^{3}H-ES with the SC sample took place in less than 12 h and that a longer incubation period might result in too fragile a membrane sample for the partitioning experiments. After 12 h, the SC sample was taken out from the solution by tweezers and blotted by Kimwipe® tissue paper. The enhancer and ES concentrations of the solution in the screw-capped glass vial were checked. The wet SC sample was carefully weighed in a

snap-capped glass bottle. Then, 5 mL of 100% ethanol was added into the bottle to extract the enhancer and ES from the sample for 48 h at room temperature with occasional gentle agitation. The extracted solution was then transferred to a screw-capped Pyrex test tube. The test tube was centrifuged at 3500 rpm for 15 min. The supernatant was analyzed for the enhancer by GC or HPLC and for ES by a scintillation counter.

The uptake amount of enhancer in the heptane-treated SC or delipidized SC was calculated as follows:

$$A_{\text{corrected},i} = \frac{A_{\text{extracted},i}}{W_{\text{dry}}} - \left(W_{\text{wet}} - W_{\text{dry}}\right)\frac{Ci}{W_{\text{dry}}} \quad (7.7)$$

where $A_{\text{extracted},i}$ is the amount enhancer extracted from heptane-treated or delipidized HMS SC, W_{dry} is the dried heptane-treated or delipidized SC weight, and the subscript i represents the enhancer. A correction for the enhancer in the aqueous compartment(s) of the SC was calculated according to the wet weight of SC (W_{wet}) and the concentration of the enhancer in aqueous bulk phase (C_i). The partition coefficient of ES (K_{ES}) for partitioning from the aqueous phase into *n*-heptane-treated SC or delipidized SC was calculated as follows:

$$K_{\text{ES}} = \frac{\left[A'_{\text{extracted}} - \left(W_{\text{wet}} - W_{\text{dry}}\right)C'_i\right]/W_{\text{dry}}}{C'_i}\frac{S'_{\text{X}}}{S'_{\text{O}}} \quad (7.8)$$

where $A'_{\text{extracted}}$ is the amount of extracted ^{3}H-ES, C'_i is the concentration of ^{3}H-ES in aqueous bulk phase, and S'_{X} and S'_{O} are the solubilities of ES in enhancer solution and in PBS, respectively. The solubility ratio corrects for any activity coefficient differences between the activity coefficient of ES in PBS and that in the enhancer solution.

7.2.3.4 Permeant Partitioning into the Transport Rate-Limiting Domain and Equilibrium Permeant Partitioning into the Stratum Corneum Intercellular Lipids

An important question raised in the above transport and equilibrium partition studies was: is the equilibrium partition enhancement data of ES a direct correlate of the partition enhancement of ES in SC permeation? To address this question, the partition enhancement in SC permeation was determined in skin transport experiments using a nonsteady state transport analysis (He et al. 2005). However, a direct comparison of the partition enhancement data obtained in transport experiments and those data obtained in equilibrium partitioning experiments of ES was not practical due to the D/E layer being a significant barrier for ES permeation across HMS. Furthermore, significant ES metabolism was observed in ES transdermal permeation. Because of these difficulties, nonsteady state ES transport analysis was complicated, and it was decided to employ CS as the surrogate permeant for ES in the following study. The strategy here was to examine the relationship between the transport partitioning enhancement of CS and the equilibrium partitioning enhancement of ES, with the assumption that ES and CS should likely behave similarly. This assumption was considered to be reasonable because previous studies had shown similar permeability coefficient enhancement effects of chemical enhancers with ES and CS for permeation across the lipoidal pathway of HMS SC (Yoneto et al. 1995).

The skin transport model (He et al. 2005) is a two-layer numerical transport simulation with a least squares-fitting software Scientist (MicroMath, Salt Lake City, UT). This model assumes that both SC and D/E are homogenous and divides the SC and D/E into a sufficient number of layers characterized by partition, diffusion, and dimension parameters. The permeant concentration in the donor chamber was assumed constant, which was true in all transport experiments carried out in the study. The receiver chamber concentration was kept at sink conditions. The transport data of full-thickness HMS were analyzed using the model to obtain the partition coefficient (K_{SC}) and diffusion coefficient (D_{SC}) of SC. The reduced parameters $K_{SC'}$ and $D_{SC'}$ of SC were then calculated:

$$D_{\text{SC}'} = D_{\text{SC}} / L^2 \quad (7.9)$$

$$K_{SC'} = K_{SC} L \quad (7.10)$$

where L is the effective path length across SC. These reduced parameters K_{SC}' and D_{SC}' were defined (Okamoto et al. 1988) to avoid the difficulty and uncertainty in assigning the L value and to minimize the number of parameters for least square fitting in model analyses of the experimental transport data. The enhancement of K_{SC}' and D_{SC}' ($E_{K,\,SC}$ and $E_{D,\,SC}$, respectively) was calculated by dividing the K_{SC}' and D_{SC}' parameters obtained with the enhancers at $E=10$ by those with PBS control.

7.3 Results and Discussion

7.3.1 Isoenhancement Concentrations and Enhancer Effects

Figure 7.2 shows a representative plot of enhancement factor vs. aqueous enhancer concentration for ES, CS, and HC permeation across the SC lipoidal pathway with 1-butyl-2-pyrrolidone, 1-hexyl-2-pyrrolidone, and 1-octyl-2-pyrrolidone as permeation enhancers (Yoneto et al. 1995). Similar enhancement factor vs. aqueous enhancer concentration plots were observed for the enhancers studied. The enhancement factor profiles at increasing aqueous enhancer concentrations are essentially the same for the steroidal permeants of different lipophilicity, suggesting the same mechanism of permeation enhancement for these steroidal permeants.

7.3.2 Effects of Alkyl Chain Length

The isoenhancement concentrations at $E=10$ for more than 20 different enhancers are presented in Fig. 7.3 (Warner et al. 2003); isoenhancement concentration is defined as the aqueous concentrations of enhancers to induce the same enhancement factor and in this case $E=10$. These isoenhancement concentrations were interpolated from the E vs. aqueous enhancer concentration plots similar to those in Fig. 7.2. Figure 7.3 shows the relationship between the $E=10$ enhancer concentration and the carbon number of the enhancer n-alkyl group (at constant permeant thermodynamic activity). The major conclusion deduced from the data in Fig. 7.3 is a slope of around −0.55 found for each enhancer series (enhancers have the same polar head functional group but different alkyl chain length) in the figure. The value of −0.55 translates into an around

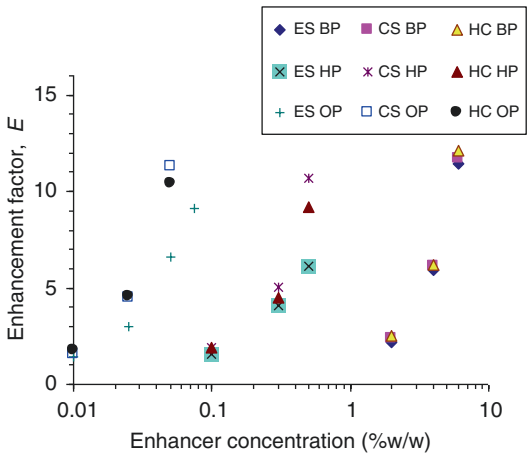

Fig. 7.2 Transport enhancement factors of estradiol (ES), corticosterone (CS), and hydrocortisone (HC) across the SC lipoidal pathway in the presence of 1-butyl-2-pyrrolidone (BP), 1-hexyl-2-pyrrolidone (HP), and 1-octyl-2-pyrrolidone (OP). The transport enhancement factors were calculated using Eq. (7.6)

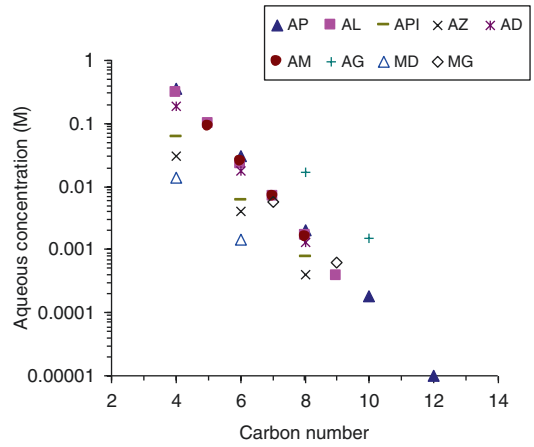

Fig. 7.3 Relationships between the aqueous $E=10$ isoenhancement concentrations of the enhancers and the carbon number of the enhancer alkyl chain. Each data point represents the average value without showing the standard deviation because the error bar generally lies within the symbol in the plot. Enhancer abbreviations are provided in Fig. 7.1

3.5-fold increase in potency per methylene group for the enhancers. In other words, the aqueous concentration required to induce $E=10$ increases 3.5-fold when the alkyl chain length of the enhancer decreases by one methylene group. The constant slope of −0.55 for the different enhancer series suggests a hydrophobic effect involving the transfer of the methylene group from the aqueous phase to a relatively nonpolar organic phase (e.g., Tanford 1980).

The results of the equilibrium partition experiments with the enhancers conducted to determine the amount of enhancers in the SC intercellular lipids under the isoenhancement $E=10$ conditions (He et al. 2003, 2004) are shown in Fig. 7.4. Note that the scale of the *y*-axis in Fig. 7.4 is the same as that in Fig. 7.3. The data in Fig. 7.4 suggest that there was little effect of the enhancer alkyl chain length upon the enhancer potency based on the concentrations of the enhancers in the intercellular lipid lamellae (relative to that based on the $E=10$ aqueous enhancer concentrations in Fig. 7.3), thus suggesting that the intrinsic potency of the enhancers at their site of action, generally believed to be the SC intercellular lipids, is relatively independent of their alkyl group chain length and lipophilicity.

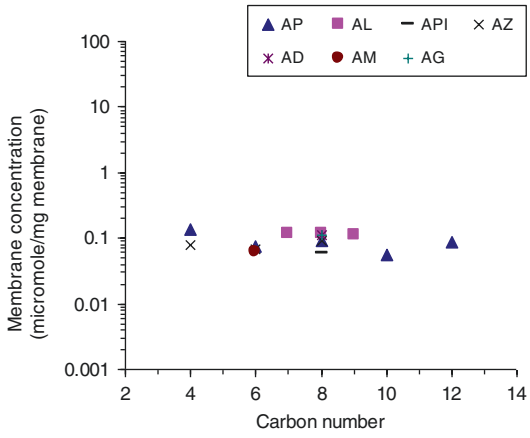

Fig. 7.4 Relationship between the enhancer concentrations in the intercellular lipid domain of the SC membrane at the $E=10$ isoenhancement conditions and the carbon number of the enhancer alkyl chain. Each data point represents the average value. Enhancer abbreviations are provided in Fig. 7.1

7.3.3 Effects of Polar Head Functional Groups

The data in Fig. 7.3 also show that some enhancer polar functional groups are more effective (more potent) than the others in inducing permeation enhancement. For example, the $E=10$ isoenhancement concentrations of 1-alkyl-2-azacycloheptanones are consistently around tenfold lower than those of 1-alkyl-2-pyrrolidones at the same *n*-alkyl chain length, suggesting that the azacycloheptanone group makes the 1-alkyl-2-azacycloheptanones more effective permeation enhancers as compared with the pyrrolidone group of the 1-alkyl-2-pyrrolidones based on their concentrations in the aqueous phase in the donor and receiver chambers. However, the relative constant concentration of enhancer uptake into the SC lipid domain at $E=10$ in Fig. 7.4 reveals that there is little effect of the enhancer polar head functional group upon the enhancer potency based on the concentrations of the enhancers at their site of action. This is an interesting finding because studies using conventional experimental methods in the literature have demonstrated the influence of the polar head functional group of an enhancer upon its effectiveness in transdermal permeation enhancement (e.g., Smith and Maibach 1995). In particular, it has been suggested that the azacycloheptanone functional group is more potent than other polar head functional groups in general due to specific interactions between the functional group and the ceramide lipid matrix (e.g., Brain and Walters 1993; Hadgraft et al. 1996). The data in Fig. 7.4, however, imply that the polar head and alkyl groups of the enhancers act only to transfer the enhancers from the aqueous phase to the hydrocarbon phase of the SC lipid lamellae and make available the enhancers for their action in the SC transport rate-limiting domain.

Figure 7.5 is a replot of the data shown in Fig. 7.3 to demonstrate a structure-enhancement relationship for the enhancers (Warner et al. 2003). The correlation between the $E=10$ isoenhancement concentrations and the octanol/PBS partition coefficients of the enhancers with a slope of around −1 suggests that the potencies of

the enhancers for the steroidal permeants are related to the enhancer lipophilicities. Together with the data analysis in Figs. 7.3 and 7.4, it is reasonable to hypothesize that (a) permeation enhancement is related to the ability of the permeation enhancer to partition into the transport rate-limiting domain in SC, (b) the polar head group assists the translocation of the enhancer to the site of action through a free energy of transfer from the bulk aqueous phase to the transport rate-limiting domain, and (c) the transport rate-limiting domain has a microenvironment with polarity similar to the polarity of bulk octanol. These hypotheses and the results of Fig. 7.5 have been discussed in detail in a recent book chapter (Li and Higuchi 2015).

7.3.4 Effects of Hydrocarbon Chain Carbon–Carbon Double Bond

The effects of substituting a single carbon–carbon bond on the *n*-alkyl chain of an enhancer with a carbon–carbon double bond have been investigated, and the $E=10$ isoenhancement concentrations of the *cis*-and *trans*-3-alken-1-ols (closed symbols) are plotted against the carbon numbers of the enhancer hydrocarbon chains in Fig. 7.6 (He et al. 2004). The data for the *n*-alkanols reported in Fig. 7.3 are also included in Fig. 7.6 for comparison. In Fig. 7.6, it is seen that the $E=10$ isoenhancement concentrations of the *cis*- and *trans*-3-alken-1-ols are two to three times higher than those of the corresponding *n*-alkanols (open squares). Based on the criterion that the $E=10$ isoenhancement (aqueous) concentration is a measure of the enhancer potency, the results in Fig. 7.6 would suggest the *cis*- and *trans*-3-alken-1-ols are less potent than the *n*-alkanols by a factor of 2 to 3. However, when the $E=10$ isoenhancement concentrations of the *cis*- and *trans*-3-alken-1-ols and of the *n*-alkyl enhancers are plotted against their octanol/PBS partition coefficients ($K_{octanol/PBS}$) in Fig. 7.7, the *cis*- and *trans*-3-alken-1-ol data fall closely on the correlation line in the figure (same correlation line as that in Fig. 7.5) when the lipophilicity of the enhancers is taken into consideration. The correlation between the $E=10$ isoenhancement concentration and octanol/PBS partition coefficient here is consistent with the demonstrated structure–enhancement relationship for the *n*-alkyl enhancers in Fig. 7.5.

In the equilibrium partition experiments of the *cis*- and *trans*-3-alken-1-ols, the concentrations of the enhancers in the SC intercellular lipid

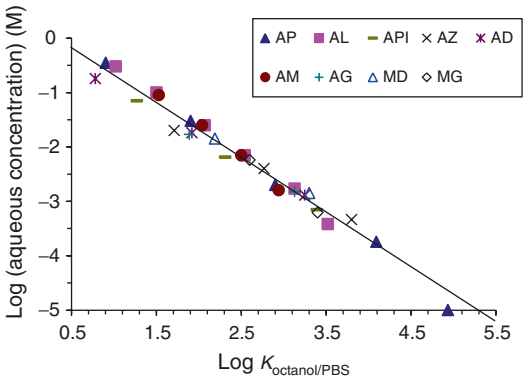

Fig. 7.5 Correlation between the aqueous $E=10$ isoenhancement concentration of the enhancer and its octanol/PBS partition coefficient ($K_{octanol/PBS}$). The slope of the line is −1. Each data point represents the average value without showing the standard deviation because the error bar generally lies within the symbol in the plot. Enhancer abbreviations are provided in Fig. 7.1

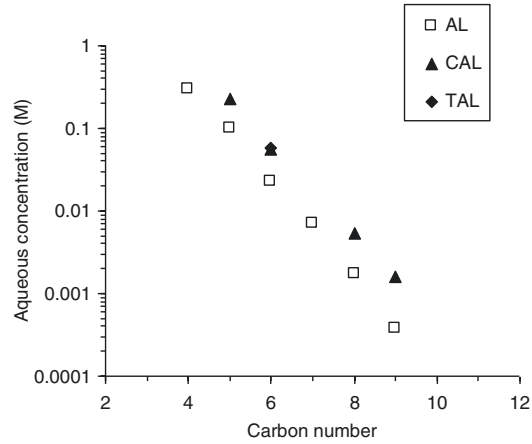

Fig. 7.6 Relationships between the aqueous $E=10$ isoenhancement concentrations of the enhancers and the carbon number of the enhancer alkyl chain. Each data point represents the average value without showing the standard deviation because the error bar generally lies within the symbol in the plot. Enhancer abbreviations are provided in Fig. 7.1

domain under the isoenhancement $E=10$ conditions are essentially constant (Fig. 7.8). The substitution of a single carbon–carbon bond with a carbon–carbon double bond on the alkyl chain here has little effect upon the enhancer potency based on the concentrations of the enhancers in the SC intercellular lipid domain. This is somewhat surprising because enhancers with unsaturated hydrocarbon chains are expected to be more potent than enhancers with saturated hydrocarbon chains based on molecular modeling of skin permeation and previous experimental results (Golden et al. 1987; Aungst 1989; Brain and Walters 1993; Tenjarla et al. 1999).

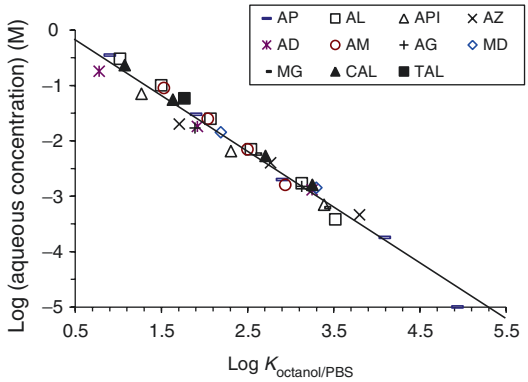

Fig. 7.7 Correlation between the aqueous $E=10$ isoenhancement concentration of the enhancer and its octanol/PBS partition coefficient ($K_{octanol/PBS}$). Each data point represents the average value without showing the standard deviation because the error bar generally lies within the symbol in the plot. The slope of the line is −1. Enhancer abbreviations are provided in Fig. 7.1

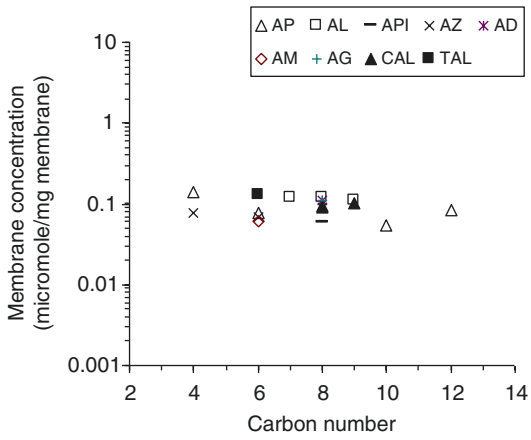

Fig. 7.8 Relationship between the enhancer concentrations in the intercellular lipid domain of the SC membrane at the $E=10$ isoenhancement conditions and the carbon number of the enhancer alkyl chain. Each data point represents the average value. Enhancer abbreviations are provided in Fig. 7.1

7.3.5 Effects of Branched Alkyl Chain

Branched chain alkanols (2-alkanols, 3-alkanols, 4-alkanols, and 5-nonanol) were also investigated as another group of skin permeation enhancers to provide insights into the mechanism of action of both *n*-alkyl and branched chain enhancers (Chantasart et al. 2004). The 2-alkanols, 3-alkanols, and 4-alkanols are 2-hexanol, 2-heptanol, 2-octanol, 2-nonanol; 3-hexanol, 3-heptanol, 3-octanol, 3-nonanol; and 4-heptanol, 4-octanol, and 4-nonanol, respectively. In Fig. 7.9, the isoenhancement concentrations at $E=10$ of the branched alkanols (closed symbols) are plotted against their $K_{octanol/PBS}$ values. Again, the data of the *n*-alkyl enhancers (including the *n*-alkanols) are included in Fig. 7.9, and the straight line shown in the figure is a best fit line based on the data for more than 20 *n*-alkyl enhancers in Fig. 7.5. Different from the random deviations for the *n*-alkyl enhancers (crosses), the

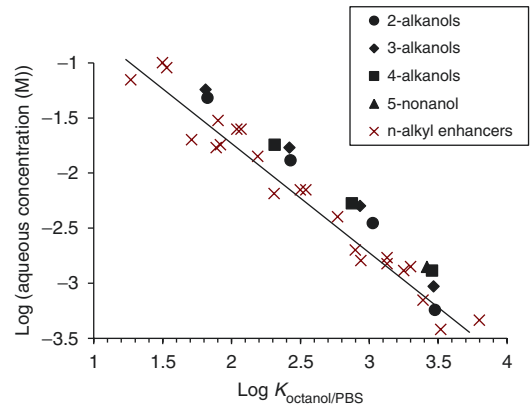

Fig. 7.9 Correlation between the aqueous $E=10$ isoenhancement concentration of the enhancer and its octanol/PBS partition coefficient ($K_{octanol/PBS}$). Each data point represents the average value without showing the standard deviation because the error bar generally lies within the symbol in the plot. The slope of the line is −1

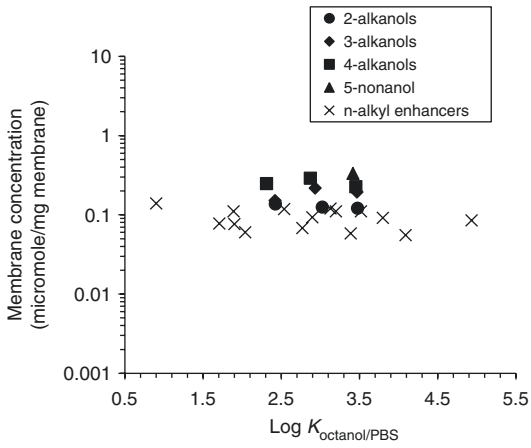

Fig. 7.10 Relationship between the enhancer concentrations in the intercellular lipid domain of the SC membrane at the $E=10$ isoenhancement conditions and the octanol/PBS partition coefficient ($K_{octanol/PBS}$) of the enhancers. Each data point represents the average value

branched chain alkanols (closed symbols) show modest but consistent positive deviations (in the direction of lower potency) from the quantitative structure–enhancement correlation (the straight line). These deviations support the view, based on the assumption that $K_{octanol/PBS}$ is a valid predictor of enhancer potency, that the branched chain alkanols are slightly less potent than the *n*-alkyl enhancers. The lower potencies based on the $E=10$ aqueous concentrations of the branched chain alkanols could be attributed to decreasing intrinsic potency and increasing effective hydrophilicity of the enhancers when the hydroxyl group moves from the terminal end towards the center of the enhancer alkyl chain. Nevertheless, the results of the branched chain alkanols continue to support the hypothesis previously established for the *n*-alkyl enhancers that the potency of an enhancer based on its aqueous concentration increases with enhancer lipophilicity.

Figure 7.10 presents the concentrations of the branched chain alkanols and *n*-alkyl enhancers in the SC intercellular lipids under the isoenhancement conditions of $E=10$. Whereas the intrinsic potencies of the *n*-alkyl enhancers are essentially the same and independent of their alkyl chain length, branching of the alkyl chain decreases the intrinsic potencies of the enhancers; the concentrations of the branched alkanols in the SC intercellular lipid domain (closed symbols) required to induce the $E=10$ conditions are generally higher than those of the *n*-alkyl enhancers (crosses in the figure). This result is consistent with the relatively lower intrinsic potency of the branched chain alkanols suggested with the data in Fig. 7.9.

Despite the observed deviation of the branched chain alkanols from the *n*-alkyl chain enhancers, it should be noted that the correlation between the logarithm of the enhancer partition coefficient from the aqueous phase to the SC intercellular lipid phase (log $K_{SC\ lipid/PBS}$) and log $K_{octanol/PBS}$ continues to hold for the branched chain alkanols. The microenvironment of the enhancer site of action remains essentially the same and independent of alkyl-chain branching; the *n*-alkanols, branched chain alkanols, and all other studied enhancers fall on the same regression line (Fig. 5.9 in a recent book chapter; Li and Higuchi 2015).

7.3.6 Equilibrium Partition Enhancement of ES into SC Intercellular Lipids

In addition to the equilibrium partition experiments of the enhancers, experiments were also conducted with a model steroidal compound ES (He et al. 2003, 2004; Chantasart et al. 2004). The goal here was to determine the enhancement of the partitioning of a lipophilic permeant into the SC intercellular lipids under the isoenhancement $E=10$ conditions. Figure 7.11 shows the plots of the partition coefficients of ES from the aqueous phase into the SC intercellular lipid domain (K_{ES}) under the $E=10$ conditions of more than 20 different enhancers vs. the $K_{octanol/PBS}$ values of the enhancers. The K_{ES} values were determined with Eq. (7.8). The dotted line represents the K_{ES} value in PBS control. As can been seen in the figure, approximately the same enhancement of K_{ES} (four- to sevenfold) was induced under the isoenhancement conditions of $E=10$ for all the enhancers studied. The relatively constant four- to sevenfold enhancement in permeant partitioning suggests that (a) the same target site in the SC

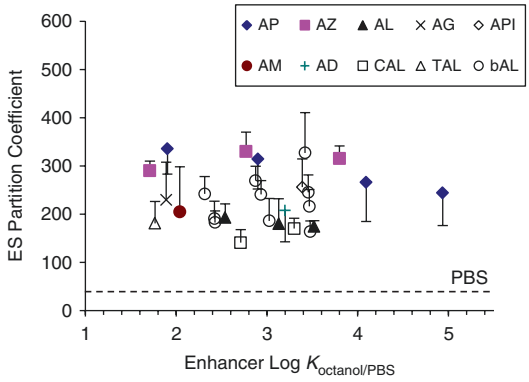

Fig. 7.11 Relationship between the partition coefficients of ES (K_{ES}) for partitioning from the aqueous phase into the SC intercellular lipid domain and the enhancer octanol/PBS partition coefficients ($K_{octanol/PBS}$). The dotted line represents the K_{ES} value in PBS control. Each data point represents the average and its standard deviation ($n>3$). The standard deviations of Log $K_{octanol/PBS}$ are not shown because the error bars generally lie within the symbols in the plot. Enhancer abbreviations are provided in Fig. 7.1

lipid lamellae is fluidized by the studied enhancers, (b) the uptake domain probed in these partitioning studies is at the same time the transport rate-limiting domain and the enhancer site of action, and (c) the tenfold permeation enhancement corresponds to around a 4- to 7-fold and 1.5- to 2.5-fold enhancement in permeant partitioning and diffusion, respectively, in the transport rate-limiting domain.

7.3.7 Transport Rate-Limiting Domain and Equilibrium Partitioning Domain

It would be inappropriate to conclude that the uptake domain probed in the equilibrium partitioning experiments is at the same time the transport rate-limiting domain and the enhancer site of action with only the K_{ES} data above. Comparison of the partition enhancement in permeant transport across the SC rate-limiting domain and the partition enhancement in the equilibrium partition experiments is required. Consistent enhancer effects upon transport and equilibrium partitioning would suggest that the SC intercellular lipid domain probed in the partitioning experiments is the same as the transport rate-limiting domain for permeation across SC.

As described in the Experimental section, the cumulative amount of CS transported across HMS vs. time profiles in CS transport experiments were analyzed with a transport model to obtain the least squares-fitting K_{SC}' and D_{SC}' of CS in PBS, 1-octyl-2-pyrrolidone (OP), and 1-hexyl-2-azacycloheptanone (HAZ) (He et al. 2005). The least squares fittings of the CS transport data were satisfactory, and the results show that the enhancement of permeant partitioning into the transport rate-limiting domain of HMS is significantly higher than the enhancement of permeant diffusion coefficient in the domain. When the total flux enhancement (E) was 12 for OP, $E_{K,\,SC}$ was 6.0 ± 1.9 and $E_{D,\,SC}$ was 1.8 ± 0.9 (mean $\pm$ SD, $n\geq3$). For HAZ with E of 11, $E_{K,\,SC}$ was 7.9 ± 2.8 and $E_{D,\,SC}$ was 1.3 ± 0.6 (mean $\pm$ SD, $n\geq3$). This suggests that the transport enhancement of CS was mainly driven by partition enhancement in the rate-limiting domain of SC. The consistency between the partitioning enhancement of transport found with the SC rate-limiting domain ($E_{K,\,SC}$ around 6–8) and the equilibrium partitioning enhancement of ES with the SC intercellular lipids (in the range of 4–7) is quite significant. This finding provides quantitative evidence that the rate-limiting domain for the transport of the model permeants through the SC lipoidal pathway and the intercellular lipid domain probed in the equilibrium partitioning experiments have similar properties regarding the partitioning enhancement effects of chemical permeation enhancers upon the lipophilic model permeants and therefore that these domains are likely to be the same. This result also supports the conclusions on quantitative structure enhancement relationship of enhancers presented in a recent book chapter (Li and Higuchi 2015).

7.3.8 Effects of Permeation Enhancement on Permeants of Different Molecular Sizes

Most of the work so far presented in this chapter was based on the data of a single model steroidal permeant CS. Two other steroidal permeants HC

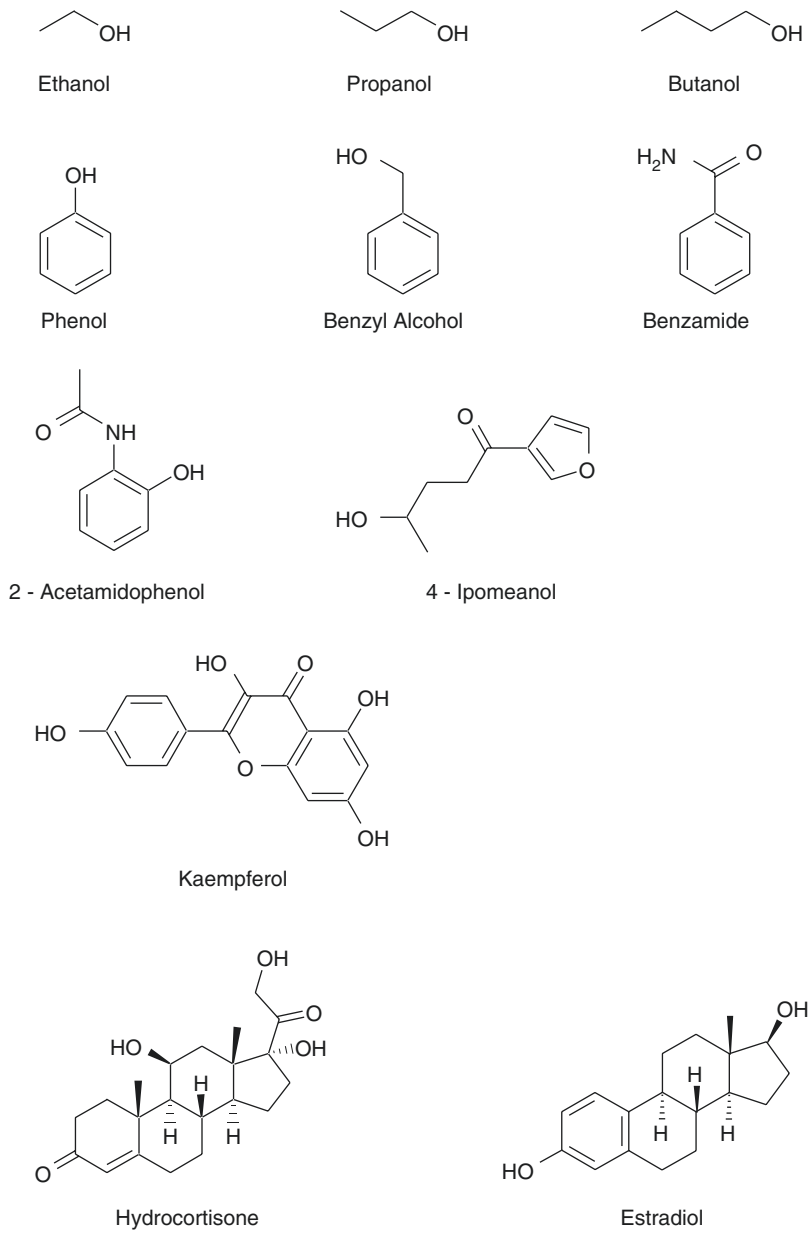

Fig. 7.12 Chemical structures of the probe permeants

and ES were also employed to examine the generality of the transport enhancement results, and essentially the same permeation enhancement was observed with all three steroidal permeants (e.g., Fig. 7.2). However, the physiochemical properties of a permeant can influence the transport of the permeant across SC. For example, it is general knowledge that there may be a steep-permeant molecular size dependence in permeation across lipid bilayers (e.g., Stein 1986; Xiang and Anderson 1994), and when enhancers fluidize the SC lipids, the increase in the bilayer free volume can have different consequences on transport enhancement of permeants with different molecular sizes (Mitragotri 2001).

To examine the effects of permeant molecular size upon transport enhancement, transport experiments were conducted using permeants of different molecular sizes and lipophilicities (Fig. 7.12) under the $E = 10$ enhancer conditions

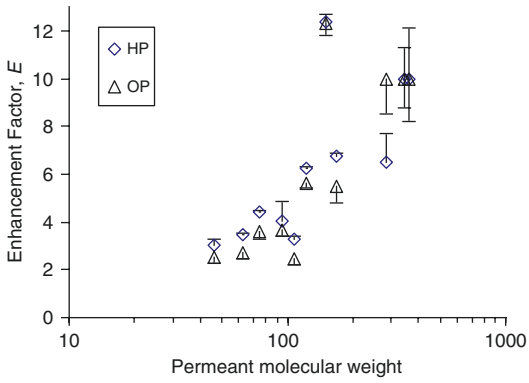

Fig. 7.13 Relationship between the transport enhancement factors and the molecular weight of the permeants under the $E=10$ condition for the steroidal permeants with 1-hexyl-2-pyrrolidone (HP) or 1-octyl-2-pyrrolidone (OP) as the enhancers. Each data point represents the average and its standard deviation ($n>3$)

for CS (Warner 2003). 1-Hexyl-2-pyrrolidone (HP) and OP were the model permeation enhancers in this study. Figure 7.13 presents the results of the enhancement factors of transport across the SC lipoidal pathway vs. the molecular weight of the permeants under the isoenhancement conditions: $E=10$ for steroidal permeants. The enhancement factors are calculated using Eqs. (7.4 and 7.6) and with the assumption that the presence of the enhancers did not affect the thermodynamic activities of the permeants in the aqueous solution. As discussed earlier, the enhancement factors for ES, CS, and HC are essentially the same in Fig. 7.13. However, there is a strong permeant molecular weight dependence upon permeation enhancement. This strong molecular weight dependence is consistent with an enhancer-induced increase in the free volume of the SC intercellular lipids, which favors the transport enhancement of permeants of large molecular sizes. The effect of permeant lipophilicity upon permeation enhancement was minimal, and no significant dependency between permeation enhancement and permeant lipophilicity was observed among the studied permeants (provided that the SC lipoidal pathway is the dominant transport pathway for permeation). Given the results in Fig. 7.13, caution needs to be exercised in generalizing the results presented in this chapter to permeants of different physicochemical properties. Further investigation on this subject is required.

7.3.9 Permeation Enhancers in a Nonaqueous System in Transdermal Drug Delivery

Although the studies presented in this chapter did not include nonaqueous vehicles or conventional cosolvents, the conclusions derived from these experiments are expected not to be limited only to the aqueous system. First, unless the vehicle is able to partition into the SC intercellular lipid "phase" and itself behaves as an enhancer, a nonaqueous system should not affect the intrinsic potency of the enhancer. In this scenario, the nonaqueous vehicle or cosolvent may only alter the thermodynamic activity of the enhancer in the dosage form such as a transdermal patch and alter the partitioning tendency of the enhancer from the patch vehicle into the SC. The concentration of the enhancer at its site of action may therefore be lowered or raised, but this effect can be predicted from thermodynamics. Further discussion can be found in a recent book chapter (Li and Higuchi 2015).

Another important issue is the symmetric situation with the enhancers in equilibrium with skin in our study of permeation enhancers. In transdermal drug delivery, enhancer permeation occurs across the SC from the transdermal patch to the blood sink, this resulting in an asymmetric enhancer situation with an enhancer concentration gradient in the SC. This enhancer concentration gradient is related to the permeability coefficients P_{SC} and $P_{D/E}$ of the enhancer. For illustrative purposes, Fig. 7.14 qualitatively shows the SC concentration gradients of two enhancers with different lipophilicities and permeability coefficients across the SC. As can be seen in the figure, the absorption of the more lipophilic enhancer (Enhancer A) is largely dermis-controlled and therefore exhibits a relatively constant concentration across the SC compared with that of the other enhancer (Enhancer B). For Enhancer B, due to its relatively low

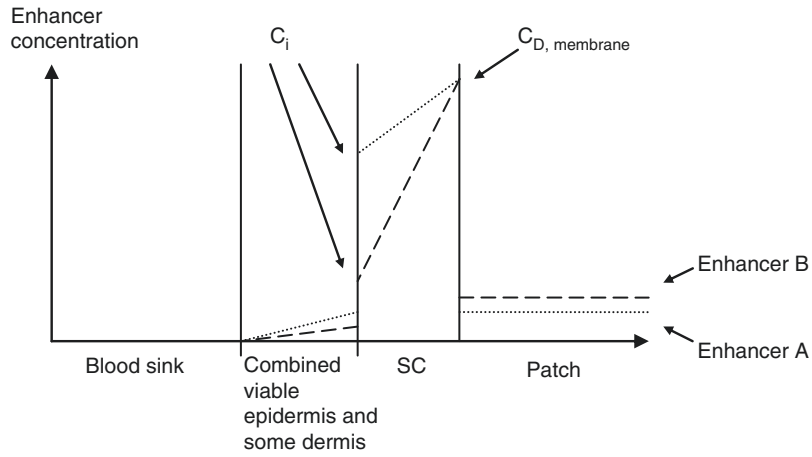

Fig. 7.14 Enhancer concentration profiles in SC in transdermal drug delivery (see Eq. 7.2): dotted line, Enhancer A; dashed line, Enhancer B. $P_{D/E}$ for Enhancers A and B are the same, log $K_{octanol/PBS}$ for Enhancer A > Enhancer B, and P_{SC} for Enhancer A > Enhancer B. This analysis assumes SC is homogenous and does not account for (*a*) enhancer-induced variation in local enhancement (permeation and partition enhancement) at different locations within the SC and (*b*) enhancer-induced enhancement for the enhancer. Such enhancement will affect the enhancer concentration in SC and lead to nonlinear profiles

permeability across the SC, a much more significant concentration drop across the SC is observed. Thus, a large portion of the SC is not affected by Enhancer B and this region of the SC becomes the rate-limiting barrier for drug transport. The relatively constant concentration of Enhancer A in the SC would suggest that lipophilic enhancers are likely to be more effective in providing uniform transport enhancement over the entire SC and a high overall flux enhancement of drug transport across SC. However, simply applying the most lipophilic enhancer does not guarantee success. The solubility of the enhancer and depletion of the enhancer in the transdermal patch are other factors that need to be considered.

The appropriateness of extrapolating the permeation experiment findings under the symmetric and equilibrium enhancer configuration to the asymmetric situation in practice has been examined in a recent study (Chantasart and Li 2010). In this study, the effects of enhancers upon the permeation of CS across HEM under the symmetric and asymmetric configurations were compared. The data show a correlation between transdermal permeation enhancement under the symmetric and asymmetric configurations. This suggests that the mechanisms of the enhancers for skin permeation under the symmetric and asymmetric configurations are likely to be the same and supports the utility of the findings in the symmetric transport studies for skin permeation under the asymmetric configurations in practice.

Conclusion

New insights into the factors influencing the effectiveness of chemical permeation enhancers for the lipoidal pathway of the SC have been obtained. The present study supports the view that (a) the potency of an *n*-alkyl enhancer (based on its aqueous concentration) is related to the enhancer lipophilicity, this being the case because of the lipophilic nature of the enhancer site of action, which is well mimicked by liquid *n*-octanol; (b) the intrinsic potency of the enhancer (as represented by its concentration at the target site of action) is relatively independent of its lipophilicity; (c) the substitution of a carbon–carbon single bond on the hydrocarbon chain of the enhancer with a carbon–carbon double bond does not significantly affect its intrinsic potency; and (d) with modest effects, branching of the *n*-alkyl chain of the enhancer generally

reduces the intrinsic potency of the enhancer. To date, we have not encountered any enhancer candidates that are inconsistent with this view in our research. However, skin penetration retarders have been reported (e.g., Hadgraft et al. 1996). This suggests that further studies are needed for greater generalization of the present findings. Nevertheless, the present study has demonstrated useful concepts and effective methodologies for mechanistic studies of chemical permeation enhancers.

Acknowledgments The authors thank Drs. Kevin S. Warner, Ning He, Doungdaw Chantasart, and Sarah A. Ibrahim for their contributions in the project and the financial support by NIH Grants GM 043181 and GM 063559.

References

Abrams K, Harvell JD, Shriner D, Wertz P, Maibach H, Maibach HI, Rehfeld SJ (1993) Effect of organic solvents on *in vitro* human skin water barrier function. J Invest Dermatol 101:609–613

Aungst BJ (1989) Structure/effect studies of fatty acid isomers as skin penetration enhancers and skin irritants. Pharm Res 6:244–247

Brain KR, Walters KA (1993) Molecular modeling of skin permeation enhancement by chemical agents. In: Walters KA, Hadgraft J (eds) Pharmaceutical skin penetration enhancement. Marcel Dekker, New York, pp 389–416

Chantasart D, Li SK (2010) Relationship between the enhancement effects of chemical permeation enhancers on the lipoidal transport pathway across human skin under the symmetric and asymmetric conditions *in vitro*. Pharm Res 27:1825–1836

Chantasart D, Li SK (2012) Structure enhancement relationship of chemical penetration enhancers in drug transport across the stratum corneum. Pharmaceutics 4:71–92

Chantasart D, Li SK, He N, Warner KS, Prakongpan S, Higuchi WI (2004) Mechanistic studies of branched-chain alkanols as skin permeation enhancers. J Pharm Sci 93:762–779

Chantasart D, Sa-Nguandeekul P, Prakongpan S, Li SK, Higuchi WI (2007) Comparison of the effects of chemical permeation enhancers on the lipoidal pathways of human epidermal membrane and hairless mouse skin and the mechanism of enhancer action. J Pharm Sci 96:2310–2326

Golden GM, McKie JE, Potts RO (1987) Role of stratum corneum lipid fluidity in transdermal drug flux. J Pharm Sci 76:25–28

Grubauer G, Feingold KR, Harris RM, Elias PM (1989) Lipid content and lipid type as determinants of the epidermal permeability barrier. J Lipid Res 30:89–96

Hadgraft J (2001) Modulation of the barrier function of the skin. Skin Pharmacol Appl Skin Physiol 14(Suppl 1): 72–81

Hadgraft J, Peck J, Williams DG, Pugh J, Allan G (1996) Mechanisms of action of skin penetration enhancers/retarders: azone and analogues. Int J Pharm 141:17–25

He N, Li SK, Suhonen TM, Warner KS, Higuchi WI (2003) Mechanistic study of alkyl azacycloheptanones as skin permeation enhancers by permeation and partition experiments with hairless mouse skin. J Pharm Sci 92:297–310

He N, Warner KS, Chantasart D, Shaker DS, Higuchi WI, Li SK (2004) Mechanistic study of chemical skin permeation enhancers with different polar and lipophilic functional groups. J Pharm Sci 93:1415–1430

He N, Warner KS, Higuchi WI, Li SK (2005) Model analysis of flux enhancement across hairless mouse skin induced by chemical permeation enhancers. Int J Pharm 297:9–21

Ibrahim SA, Li SK (2009a) Effects of chemical enhancers on human epidermal membrane: structure-enhancement relationship based on maximum enhancement (E_{max}). J Pharm Sci 98:926–944

Ibrahim SA, Li SK (2009b) Effects of solvent deposited enhancers on transdermal permeation and their relationship with Emax. J Control Release 136:117–124

Kim YH, Ghanem AH, Higuchi WI (1992) Model studies of epidermal permeability. Semin Dermatol 11: 145–156

Kligman AM, Christophers E (1963) Preparation of isolated sheets of human stratum corneum. Arch Dermatol 88:702–705

Lambert WJ, Higuchi WI, Knutson K, Krill SL (1989) Effects of long-term hydration leading to the development of polar channels in hairless mouse stratum corneum. J Pharm Sci 78:925–928

Lampe MA, Williams ML, Elias PM (1983) Human epidermal lipids: characterization and modulations during differentiation. J Lipid Res 24:131–140

Lee VHL, Yamamoto A, Kompella UB (1991) Mucosal penetration enhancers for facilitation of peptide and protein drug absorption. Crit Rev Ther Drug Carrier Syst 8:91–192

Li SK, Higuchi WI (2015) Quantitative structure-enhancement relationship and the microenvironment of the enhancer site of action. In: Dragicevic N, Maibach HI (eds) Percutaneous penetration enhancers, chemical methods in penetration enhancement: modification of the stratum corneum. Springer, New York, Ch. 5

Li SK, Ghanem A-H, Yoneto K, Higuchi WI (1997) Effects of 1-alkyl-2-pyrrolidones on the lipoidal pathway of human epidermal membrane: a comparison with hairless mouse skin. Pharm Res 14:S-303

Liu P, Higuchi WI, Song WQ, Kurihara-Bergstrom T, Good WR (1991) Quantitative evaluation of ethanol effects on diffusion and metabolism of beta-estradiol in hairless mouse skin. Pharm Res 8:865–872

Liu P, Higuchi WI, Ghanem A-H, Kurihara-Bergstrom T, Good WR (1992) Assessing the influence of ethanol in simultaneous diffusion and metabolism of estradiol in hairless mouse skin for the 'asymmetric' situation *in vitro*. Int J Pharm 78:123–136

Mitragotri S (2001) Effect of bilayer disruption on transdermal transport of low-molecular weight hydrophobic solutes. Pharm Res 18:1018–1023

Nicolaides N (1974) Skin lipids: their biochemical uniqueness. Science 186:19–26

Okamoto H, Hashida M, Sezaki H (1988) Structure-activity relationship of 1-alkyl or 1-alkenylazacycloalkanone derivatives as percutaneous penetration enhancers. J Pharm Sci 77:418–424

Shaker DS, Ghanem AH, Li SK, Warner KS, Hashem FM, Higuchi WI (2003) Mechanistic studies of the effect of hydroxypropyl-beta-cyclodextrin on *in vitro* transdermal permeation of corticosterone through hairless mouse skin. Int J Pharm 253:1–11

Smith EW, Maibach HI (1995) Percutaneous penetration enhancers. CRC Press, Inc., Boca Raton

Stein W (1986) Transport and diffusion across cell membranes. Academic, New York

Tanford C (1980) The hydrophobic effect: formation of micelles and biological membranes, 2nd edn. Wiley, New York

Tenjarla SN, Kasina R, Puranajoti P, Omar MS, Harris WT (1999) Synthesis and evaluation of N-acetylprolinate esters – novel skin penetration enhancers. Int J Pharm 192:147–158

Warner KS (2003) Mechanistic aspects of chemical skin permeation enhancers. PhD Thesis, University of Utah

Warner KS, Li SK, Higuchi WI (2001) Influences of alkyl group chain length and polar head group on chemical skin permeation enhancement. J Pharm Sci 90:1143–1153

Warner KS, Li SK, He N, Suhonen TM, Chantasart D, Bolikal D, Higuchi WI (2003) Structure-activity relationship for chemical skin permeation enhancers: probing the chemical microenvironment of the site of action. J Pharm Sci 92:1305–1322

Warner KS, Shaker DS, Molokhia S, Xu Q, Hao J, Higuchi WI, Li SK (2008) Silicone elastomer uptake method for determination of free 1-alkyl-2-pyrrolidone concentration in micelle and hydroxypropyl-β-cyclodextrin systems used in skin transport studies. J Pharm Sci 97:368–380

Xiang TX, Anderson BD (1994) The relationship between permeant size and permeability in lipid bilayer membranes. J Membr Biol 140:111–122

Yoneto K, Ghanem AH, Higuchi WI, Peck KD, Li SK (1995) Mechanistic studies of the 1-alkyl-2-pyrrolidones as skin permeation enhancers. J Pharm Sci 84:312–317

Yoneto K, Li SK, Higuchi WI, Shimabayashi S (1998) Influence of the permeation enhancers 1-alkyl-2-pyrrolidones on permeant partitioning into the stratum corneum. J Pharm Sci 87:209–214